Garcia-Gonzalez, D. & Hossain, M. (2021). Microstructural modelling of hard-magnetic soft materials: Dipole–dipole interactions versus Zeeman effect. *Extreme Mechanics Letters*, *48*, 101382.

DOI: 10.1016/j.eml.2021.101382

Microstructural modelling of hard-magnetic soft materials: Dipole-dipole interactions versus Zeeman effect

Daniel Garcia-Gonzalez[a,*], Mokarram Hossain[b,*]

[a]*Department of Continuum Mechanics and Structural Analysis, University Carlos III of Madrid, Avda. de la Universidad 30, 28911 Leganés, Madrid, Spain*

[b]*Zienkiewicz Centre for Computational Engineering, College of Engineering, Swansea University, SA1 8EN, United Kingdom*

Abstract

Hard-magnetic soft materials are a class of magneto-active polymers (MAPs) where the fillers are composed of hard-magnetic (magnetised) particles. These materials present complex magneto-mechanical couplings, which require the development of modelling frameworks in understanding their responses at the very beginning of conceptualisation and design. Most of the current constitutive approaches available in the literature for hard-magnetic MAPs do not consider dipole-dipole interactions of the embedded particles. However, such interactions among the magnetised particles generate internal forces within the composite that need to be balanced by mechanical stress from the polymeric matrix networks. This fact may imply an initial stretch of the polymeric network and suggests that such dipole-dipole interactions may be important during the MAP deformation process. To address these crucial points, in this contribution, we propose a novel constitutive model relating microstructural characteristics of hard-magnetic MAPs. The model accounts for polymeric network pre-stretch, dipole-dipole interactions, Zeeman effect as well as viscous mechanisms which are formulated on the finite deformation theory. The results obtained herein highlight the importance of accounting for the dipole-dipole interactions and the polymeric network pre-stretch to understand the complex magneto-mechanically coupled behaviour of hard-magnetic MAPs.

Keywords: Magneto-active polymers (MAP), Magneto-mechanics, Magnetic pre-stretch, Hard-magnetics, Microstructural model, Finite deformations

1. Introduction

Magneto-active polymers (MAPs) are a class of composite materials that mechanically respond to external magnetic stimuli. Such a response upon the action of a contactless stimuli can translate into the mechanical deformation of the MAP, changing its geometrical features, or into an alteration of its rheological properties such as stiffness and viscosity [5, 7, 8, 9]. The nature of MAP responses as a result of the magnetic stimulation largely relies on the composite internal constituents. Note that MAPs are composed of two main ingredients: a polymeric matrix and a fraction of micron-sized magnetic particles. Under the application of a magnetic field, the particles respond to the field leading to torques, attractions, and repulsive forces within the composite. These internal forces are balanced by mechanical stress from the polymeric matrix

*Corresponding authors

Email addresses: danigarc@ing.uc3m.es (Daniel Garcia-Gonzalez), mokarram.hossain@swansea.ac.uk (Mokarram Hossain)

deformation. Therefore, the nature of both polymeric matrix and magnetic particles, as well as their spatial distribution within the MAP composites, fully determines their magneto-mechanical behaviour. The polymeric matrices are ranging from very soft hydrogels to stiff thermoplastics, although in most cases the composites consist of elastomeric materials [11, 12, 21]. As expected, softer matrices result in higher mechanical deformations under the application of a magnetic field. Moreover, the type of magnetic particles determines the nature of the interactions between particles and with the external magnetic field. Depending on their magnetisation behaviour, these particles can be classified into two major groups, i.e., soft-magnetic and hard-magnetic particles [30, 31, 46].

Most of the published works to date either on experimental characterizations or computational modelling are mainly focused on MAPs manufactured with soft-magnetic particles. These particles present a low magnetic coercivity and upon removal of the applied magnetic field, they will be fully de-magnetised. When the particles are distributed within the MAP and no external magnetic field is applied, they play the same role as of other fillers used in traditional particle-filled composites. However, under the application of a magnetic field, the particles are magnetised resulting into dipole-dipole interactions between them. These internal magnetic forces are then balanced by mechanical stress from the polymeric phase, which leads to mechanical deformations within the MAP. When the external magnetic field is switched off, the particles come back to a non-magnetised state recovering the initial shape of the MAP (assuming a purely elastic nature of the underlying polymeric matrix). These materials thus allow for the remote control of their shape and mechanical properties. Such a salient feature has made soft-magnetic MAPs as excellent candidates for applications in soft robotics, shape morphing structures, and biomedical fields such as controlled drug delivery, see for example [25, 31, 43]. For an exhaustive review on experimental study of MAPs, see Bastola and Hossain [4].

Very recently, hard-magnetic MAPs (hMAPs) have become one of the most promising advanced smart materials within materials and mechanics research community. A hard-magnetic MAP consists of a polymeric matrix filled with particles that have a very high magnetic coercivity [30]. When these particles are exposed to a high enough magnetic field, they can easily reach their magnetisation saturation. Even if the external magnetic field is switched off, the particles will still present a significant magnetic remanence. This characteristic implies that hard-magnetic particles may inherit magnetisation with a different direction than the external magnetic field. In such a scenario, apart from dipole-dipole interactions, magnetic particles will also introduce torques within the MAP as they trend to align along the externally applied magnetic field direction. A pioneering work in the area is due to Zhao and co-workers [31]. In the work, they developed an additively manufacturing technique for printing filaments of hMAPs with a controlled residual magnetic flux along the filament direction. Thus, intricate magnetisation patterns can be imposed within a structural component to design programmable mechanical responses to magnetic stimuli. Other recent relevant works in this field can be consulted in Refs. [35, 32, 52, 1, 34, 49]. However, the advance in the field requires reliable modelling frameworks to help at the conceptualisation and design of hMAPs, as these materials present complex magneto-mechanical responses. A clear example of this need can be found in the recent work by Wang et al. [48], where the authors present an evolutionary design strategy by integrating theoretical modeling and the genetic algorithm. Zhao and co-authors [54] formulated a constitutive model to account for interactions between external magnetic fields and hard-magnetic particles within a finite deformation framework, which was extended further by Garcia-Gonzalez [16] to incorporate viscous deformation mechanisms associated to the polymeric component. The formulation was also followed to propose a nonlinear theory for hard-magnetic elastica, allowing thus for accurate prediction of magnetic-induced large deflections in hard-magnetic beams [47]. Regarding the micromechanical modelling of hMAPs, it has been tackled by

finite element (FE) models that incorporate the explicit definition of the composite phases, i.e., the particles and the polymeric matrix [41, 53, 40]. In addition, this microstructural modelling has also been approached by molecular dynamics simulations [44]. Another interesting approach is due to Ye et al. [51]. In this work, the authors developed a computational framework, called "Magttice", to model hMAPs with the combinations of FE scheme and lattice models.

When analysing the current state-of-the-art on hard-magnetic MAPs' modelling, we find some questions are not solved yet. One point of discussion is the relation between the spatial and material forms of magnetisation vector. Most of the previous approaches presented a given relation that modulates the material magnetisation by both rotation and stretch tensors of the deformation gradient [54, 16, 47]. However, recent computational works conducted by Danas and co-workers [39, 40] suggested that the stretch tensor does not affect the current magnetization response, which is in agreement with previous experimental observations [15]. Furthermore, to the best of the authors' knowledge, there is no lattice-based finite strain model accounting for dipole-dipole interactions between hard-magnetic particles as well as their interaction with an external field. In hMAPs, the particles are initially polarised (magnetically). This implies that dipole-dipole interactions between particles may result into MAP pre-stretch and may play a role in the mechanical response of the composite even under a null external magnetic field. This current work aims at addressing these questions from a microstructural perspective. To this end, we propose a novel constitutive model taking microstructural characteristics of hMAPs into account. The model is formulated in finite deformation settings and accounts for polymeric network pre-stretch, dipole-dipole interactions, Zeeman effect (interaction of magnetised particles with external magnetic field) and viscous mechanisms. After presenting the constitutive formulation and its numerical implementation, we use the model to analyse the importance of accounting for dipole-dipole interactions and polymeric network pre-stretch in hMAPs.

2. General magneto-mechanical constitutive framework

2.1. Kinematics and magnetic variables

In general, MAPs are highly deformable composites that stand for significant geometrical changes. To account for such large deformations and to express consistently the various kinematic quantities, we need to differentiate between the material $\mathcal{B}_0$ and spatial configurations $\mathcal{B}_t$. For this, the points of a body in the material coordinates $\boldsymbol{X}$ are designated as $\mathcal{B}_0$. Then, these points can be moved onto the spatial coordinates $\boldsymbol{x}$ in $\mathcal{B}_t$ through the nonlinear deformation map $\boldsymbol{\chi}$. This mapping process is intrinsically linked to the definition of the deformation gradient $\boldsymbol{F}$ as

$$\boldsymbol{F} = \text{Grad}\, \boldsymbol{\chi}; \quad J := \det \boldsymbol{F} > 0. \tag{1}$$

Other relevant kinematics quantities such as the left and the right Cauchy-Green tensors $\boldsymbol{b}$ and $\boldsymbol{C}$, respectively, can be derived from the deformation gradient as

$$\boldsymbol{b} := \boldsymbol{F}\boldsymbol{F}^T, \quad \boldsymbol{C} := \boldsymbol{F}^T\boldsymbol{F}. \tag{2}$$

The main variables in magneto-mechanics are the magnetic field $\mathbb{h}$, magnetisation $\mathbb{m}$, and magnetic induction $\mathbb{b}$ in the spatial configuration, while $\mathbb{H}$ and $\mathbb{B}$ are the magnetic field and magnetic induction, respectively, in the material configuration. These key variables in the two different configurations are related

by

$$\mathbb{H} = \mathbb{h}\boldsymbol{F}, \qquad \mathbb{B} = J\mathbb{b}\boldsymbol{F}^{-T}. \tag{3}$$

According to previous works [29, 13, 14], it can be concluded that there is non-uniqueness in the Lagrangian form of the magnetization variable $\mathbb{m}$. For instance, the computational work conducted by Danas and coworkers [39, 40] demonstrated that the pre-stretch does not affect the current magnetization response, which is in agreement with experimental observations [15]. This fact suggests that the magnitude of the magnetisation does not change with stretch ($\boldsymbol{U}$) but only with the rigid body rotation ($\boldsymbol{R}$) as

$$\mathbb{m} = \boldsymbol{R}\mathbb{M}, \tag{4}$$

where $\mathbb{M}$ is the initial magnetisation (residual magnetisation in the case of hMAPs) expressed in the material configuration and $\boldsymbol{R} = \boldsymbol{F}\boldsymbol{U}^{-1}$ as per the polar decomposition of the deformation gradient. This assumption has been recently evaluated by Danas and co-authors [40] for hard-magnetic MAPs demonstrating it from numerical homogenisation approaches. Note that the overall magnetisation of the material is only due to the magnetic particles as it is null within the polymeric matrix. Then, this variable is related to the summation of the magnetisations from the different particles in the volume evaluated. In MAPs, the magnetic particles are much stiffer than the matrix leading to deformations within the polymeric matrix but not to significant deformation within the particles, which only experience rigid body rotations.

2.2. Balance laws in the material configuration

The governing equations for the magnetic field $\mathbb{H}$ and the magnetic induction $\mathbb{B}$ in magneto-mechanics follow Maxwell's equations, which, in the material configuration, are defined as

$$\text{Curl}\,\mathbb{H} = \boldsymbol{0}, \quad \text{Div}\,\mathbb{B} = 0, \tag{5}$$

where, Curl and Div denote the corresponding differential operators with respect to the position vectors $\boldsymbol{X}$ in $\mathcal{B}_0$. Note that if we derive $\mathbb{H}$ from a scalar potential φ, the governing equation $(5)_1$ is automatically satisfied, i.e.,

$$\mathbb{H} = -\text{Grad}\varphi, \quad \text{in } \mathcal{B}_0. \tag{6}$$

It can be convenient to express the stress quantities either in the form of Cauchy stress $\boldsymbol{\sigma}$ defined in the spatial configuration, which is related to the first Piola-Kirchhoff stress tensor $\boldsymbol{P}$ as

$$\boldsymbol{P} = J\boldsymbol{\sigma}\boldsymbol{F}^{-T}. \tag{7}$$

2.3. Constitutive equations

In the case of isothermal processes, the strain energy function (per unit reference volume) of MAPs including time-dependent viscous responses can be expressed as a function of the deformation gradient ($\boldsymbol{F}$), an internal variable incorporating viscous response ($\boldsymbol{F}^v = \boldsymbol{F}^{-e}\boldsymbol{F}$), and a magnetic variable such as magnetic induction ($\mathbb{B}$), i.e., $\Psi\left(\boldsymbol{F}, \boldsymbol{F}^v, \mathbb{B}\right)$. Furthermore, the total energy function incorporating the contributions of the free-space in a magneto-mechanical problem can de expressed as

$$\Omega(\boldsymbol{F}, \boldsymbol{F}^v, \mathbb{B}) = \Psi(\boldsymbol{F}, \boldsymbol{F}^v, \mathbb{B}) + M_0^*(\boldsymbol{F}, \mathbb{B}), \tag{8}$$

where, $M_0^*(\boldsymbol{F}, \mathbb{B}) := -\frac{1}{2J\mu_0}[\boldsymbol{C}\mathbb{B}] \cdot \mathbb{B}$ is the component associated to the free space in the material configuration. The second law of thermodynamics in the form of Clausius-Duhem inequality becomes [10, 36]

$$\delta_0 = \boldsymbol{P} : \dot{\boldsymbol{F}} + p\boldsymbol{F}^{-T} : \dot{\boldsymbol{F}} + \mathbb{H} \cdot \dot{\mathbb{B}} - \dot{\Omega} \geq 0, \tag{9}$$

$$= \boldsymbol{P} : \dot{\boldsymbol{F}} + p\boldsymbol{F}^{-T} : \dot{\boldsymbol{F}} + \mathbb{H} \cdot \dot{\mathbb{B}} - \frac{\partial \Omega}{\partial \boldsymbol{F}} : \dot{\boldsymbol{F}} - \frac{\partial \Omega}{\partial \boldsymbol{F}_v} : \dot{\boldsymbol{F}}_v - \frac{\partial \Omega}{\partial \mathbb{B}} : \dot{\mathbb{B}} \geq 0. \tag{10}$$

Note that the term related to p (a Lagrange multiplier associated to the hydrostatic pressure) is included to impose the incompressibility condition frequently used in the case of modelling rubber-like materials [28, 42]. By applying the so-called Coleman-Noll argumentation [10], the constitutive equations can consistently be derived as

$$\boldsymbol{P} = -p\boldsymbol{F}^{-T} + \frac{\partial \Omega}{\partial \boldsymbol{F}}, \quad \mathbb{H} = \frac{\partial \Omega}{\partial \mathbb{B}}. \tag{11}$$

The remaining term $-\frac{\partial \Omega}{\partial \boldsymbol{F}_v} : \dot{\boldsymbol{F}}_v \geq 0$ adds a consistency condition to define an evolution equation for $\boldsymbol{F}_v$ in the following section. For more details on fundamental equations of magneto-mechanics, readers are referred to our recent publications [16, 24], Bustamante et al. [6], and Griffiths [20], Maugin [36].

3. Microstructural-based constitutive formulation for hard-magnetic soft materials

In this section, a constitutive formulation to define the magneto-mechanical behaviour of hard-magnetic soft materials at finite strains is devised. The formulation evaluates first the initial state of MAPs providing the mechanical balance between dipole-dipole interactions of the magnetised hard-particles and the polymeric network. Then, a microstructural-based model is presented accounting for non-linearities, dipole-dipole interactions, Zeeman effect, and time-dependent viscous mechanisms.

3.1. Conceptualisation of the model

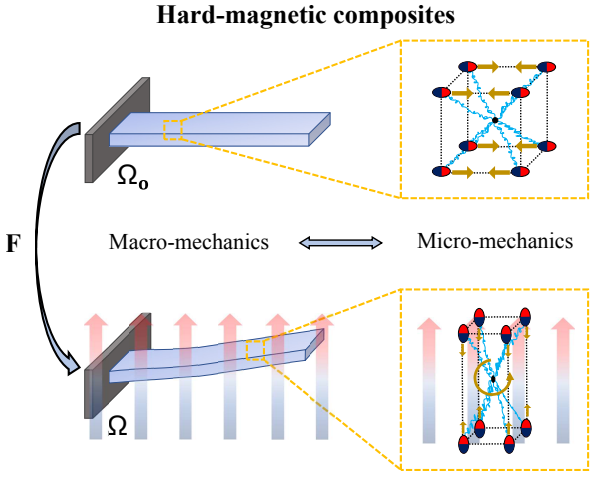

Figure 1. A schematic diagram of the hard-magnetic MAP's physics from macro- to micro-scales. Under null external magnetic field, the magnetised particles interact by means of dipole-dipole internal forces. After the application of an external magnetic field, these particles orient themself along the field direction due to an internal torque. Due to the microstructural deformations and changes in the particles' orientations, the dipole-dipole interactions also change.

For the manufacturing of hMAPs, the particles are usually subjected to a strong magnetic field during the curing process which helps reaching their saturation magnetisation and thus leading to a magnetic remanence

(i.e., a residual magnetic flux density). If the magnetic coercivity of the particles is high enough, these can withstand external magnetic fields without demagnetising. In such a scenario, when the MAP is exposed to an external magnetic field (note that this is the second time applied field, not the one applied during the curing process), the particles will tend to align along the field direction resulting into internal torques within the polymeric matrix (Figure 1). Therefore, the response of the MAP depends on a mechanical balance between external loads, the stress contribution from the deformation of the polymeric network, the magnetic dipole-dipole interactions between the particles and the magnetic torques arising from the aforementioned interaction between the magnetised particles and the external field (due to the Zeeman energy [33]).

An important point for the conceptualisation of this work relies on the nature of the manufacturing process. In this regard, two main scenarios can be envisaged. The first manufacturing option consists in filling a polymeric matrix with non-magnetised particles. For low and moderate external magnetic fields, these particles will be magnetised and, when the field is removed, they will be fully de-magnetised. These type of MAPs can be produced either as homogenised composites or MAPs with a preferred direction. In the latter case, a magnetic field is applied during the curing process [22, 23]. After the curing and solidification, a strong magnetic field can be applied to MAPs until reaching the magnetic saturation and, if the particles have a high enough coercivity, these will present a given magnetic remanence. Such magneto-mechanically coupled scenarios can be modelled following our recently proposed microstructural-based approach by introducing magnetic hysteresis in a "plastic-like" fashion [18]. The model can simulate the evolution of the MAP deformation state during the magnetisation process accounting for dipole-dipole interactions between particles until reaching the saturation, and provides the final deformation and magnetic state of the MAP. Note that the aforementioned homogenised MAPs can also be synthesised using already magnetised particles without applying any magnetic during the curing process. For such a hard-magnetic composite, our previously proposed model [18] can be used just by adding a torque term in the energy function as proposed by Zhao and co-workers [54].

Now, we want to develop a constitutive model for hard-magnetic soft composites in which a second way of the manufacturing method is considered. In this case, a strong external magnetic field is applied during the curing process of MAPs embedded with hard-magnetic particles. Such a composite can be produced either using a traditional synthesis process or using an advanced additive manufacturing/3D printing technique, e.g. the 3D printing technique proposed by Zhao group [54]. In the latter case, the (hard) magnetic particles will align along the applied magnetic field direction leading to chain-like distributions. Most importantly, during the curing process, the magnetisation that the particles will develop will not be de-magnetised even after the removal of the applied field. This magnetisation is called the magnetic remanence or the residual magnetisation. The resulting MAP after curing, even under null external mechanical and magnetic conditions (i.e., stress-free conditions), presents a given reference volume with a corresponding homogenised deformation state given by $\boldsymbol{F} = \boldsymbol{I}$ (with $\boldsymbol{I}$ being the second order unit tensor). However, hard-magnetic particles have a remanent magnetisation which implies some dipole-dipole interactions leading to internal magnetic stress within the composite. This magnetic stress needs, therefore, to be balanced by the deformation of the polymeric network part of the composite. As a consequence, although the resulting MAP as a whole can be conceptualised as a non-deformed solid, its microstructural phases present some pre-stretch components. Note that such a polymeric network deformation will strongly depend on the curing time scale and the ease of particles' motion within the uncured matrix. In the following, we present a novel constitutive framework to account for such pre-stretch conditions along with the main relevant magneto-mechanical mechanisms playing a role in hMAPs manufactured under a magnetic field during the curing process.

3.2. Magneto-mechanical balance at reference configuration: initial pre-stretch field

The current approaches in the literature consider MAPs as initially relaxed materials in which the magnetic particles are distributed within a non-stretched polymeric network. This assumption is completely valid for MAPs reinforced with soft-magnetic particles (e.g., carbonyl iron particles). Such particles present null magnetic polarisation under a null external magnetic field. If a magnetic field is applied after the solidification process, the magnetisation of soft-magnetic particles evolves leading to internal repulsive/attraction forces that result into the overall deformation of the MAP. However, when the MAP is reinforced with hard-magnetic particles that are aligned during the solidification process, there exists initial magnetisation in the composite which will create some internal magnetic forces. This effect has indirectly been observed in molecular dynamic simulations and is directly derived by the nature of magnetised particles and dipole-dipole interactive forces [44]. It implies that, for a hMAP, even in the initial equilibrium (without any external mechanical or magnetic load), the polymeric network must undergo some pre-stretches to fulfil the mechanical balance compensating the magnetic forces with a polymeric pre-stress.

However, most of the currently available constitutive models for hMAPs do not consider the aforementioned physical consistency. Hence, we devise a coupled constitutive formulation on the basis of two deformation gradient tensors: the total deformation tensor of the hMAP ($\boldsymbol{F}$); and the microstructural deformation tensor of the polymeric network ($\boldsymbol{F}_{\text{pn}}$). For purely elastic-recoverable deformation processes, both tensors are related by a pre-deformation tensor ($\boldsymbol{F}_{\text{pn}}^{0}$), whose physical meaning relates to the inverse of the initial stretch state of the polymeric network, as

$$\boldsymbol{F} = \boldsymbol{F}_{\text{pn}}\boldsymbol{F}_{\text{pn}}^{0}. \tag{12}$$

However, due to the viscoelastic nature of the underlying polymeric matrix, the deformation gradient can present certain viscous contribution. In such a scenario, the components of the polymeric network deformation gradient will further be decomposed as

$$\boldsymbol{F} = \boldsymbol{F}_{\text{pn}}\boldsymbol{F}_{\text{pn}}^{0} = \boldsymbol{F}_{\text{pn}}^{e}\boldsymbol{F}_{\text{pn}}^{v}\boldsymbol{F}_{\text{pn}}^{0} \tag{13}$$

where, $\boldsymbol{F}_{\text{pn}}^{e}$ and $\boldsymbol{F}_{\text{pn}}^{v}$ are elastic and viscous contributions of the polymeric network deformation gradient, respectively. Therefore, the mechanical contribution to the energy potential associated to the polymeric network component can directly be written by means of

$$\begin{aligned} \boldsymbol{F}_{\text{pn}} &= \boldsymbol{F}\boldsymbol{F}_{\text{pn}}^{-0} \\ \boldsymbol{F}_{\text{pn}}^{e} &= \boldsymbol{F}\boldsymbol{F}_{\text{pn}}^{-0}\boldsymbol{F}_{\text{pn}}^{-v}. \end{aligned} \tag{14}$$

Details on the numerical computation of this tensor for specific distribution and properties of the magnetic particles within the polymeric matrix are provided in Section 3.4.

3.3. Magneto-mechanical constitutive formulation

The constitutive formulation is conceptualised as the combination of the microstructural contributions of the polymeric network and the hard-magnetic particles. The vacuum permeability of the free space term $M_0^*(\boldsymbol{F}, \mathbb{B})$ is assumed negligible [37]. To facilitate the definition of the different magneto-mechanical responses of MAP, we devise a total Helmholtz free energy function (Ψ) as the addition of mechanical

(Ψ_{mech}) and magnetic (Ψ_{mag}) terms, i.e.,

$$\Psi\left(\boldsymbol{F}, \boldsymbol{F}_{\text{pn}}^{v}, \mathbb{B}\right) = \Psi_{\text{mech}}\left(\boldsymbol{F}, \boldsymbol{F}_{\text{pn}}^{v}\right) + \Psi_{\text{mag}}\left(\boldsymbol{F}, \mathbb{B}\right). \tag{15}$$

Note that, although the tensor $\boldsymbol{F}_{\text{pn}}^{0}$ is not an independent variable, the complete definition of the problem requires the computation of the pre-deformation tensor of the polymeric network from the initial magneto-mechanical properties. Similarly, the complete definition of the problem also requires the local magnetisation of the hard-magnetic particles ($\mathbb{M}$) and their spatial distribution. These potential energy definitions can further be decomposed into the specific mechanical and magnetic responses. To this end, the total mechanical energy function is divided as

$$\Psi_{\text{mech}}\left(\boldsymbol{F}, \boldsymbol{F}_{\text{pn}}^{v}\right) = \Psi_{\text{mech}}^{e}\left(\boldsymbol{F}\right) + \Psi_{\text{mech}}^{v}\left(\boldsymbol{F}, \boldsymbol{F}_{\text{pn}}^{v}\right) \tag{16}$$

where, Ψ_{mech}^{e} is an equilibrium component (i.e., purely elastic and rate-independent term) and Ψ_{mech}^{v} is a non-equilibrium component (i.e., viscous and rate-dependent term). Regarding the magnetic contribution, it can be decomposed into two terms

$$\Psi_{\text{mag}}\left(\boldsymbol{F}, \mathbb{B}\right) = \Psi_{\text{mag}}^{\text{d-d}}\left(\boldsymbol{F}\right) + \Psi_{\text{mag}}^{\text{z}}\left(\boldsymbol{F}, \mathbb{B}\right) \tag{17}$$

where, $\Psi_{\text{mag}}^{\text{d-d}}$ represents the magnetic potential related to the so-called dipole-dipole interactions and must depend on the particles' magnetisation upon an external magnetic field and spatial distribution as a result of mechanical and magnetic loads; and $\Psi_{\text{mag}}^{\text{z}}$ represents the potential function related to the hard-magnetic response, i.e., Zeeman potential energy due to the application of an external field $\mathbb{B}$ on an already magnetised solid (magnetisation induced during the curing process) [33]. The physical meaning of these two contributions is explained in Section 3.1 and further detailed in the following sections.

3.3.1. Mechanical strain energy functions and stress derivation

The mechanical contribution to the free energy has to account for the overall response of the MAP considering both polymeric network and magnetic particles. To this end, the polymeric network is defined as visco-hyperelastic in nature while the magnetic particles contribute to the apparent stiffness of the purely hyperelastic response. Therefore, according to Eqn (16), the mechanical free energy can be decomposed into a rate-independent (elastic) contribution accounting for both polymeric network and magnetic particles components, and a rate-dependent (viscous) contribution accounting only for the polymeric network. Note that according to Section 3.2, to fulfil the mechanical balance condition, the polymeric network must be initially pre-stretched to compensate the dipole-dipole interactions of the hard-magnetic particles that are induced during the curing process under an external magnetic field. Therefore, the mechanical free energies must be expressed by means of the actual polymeric network deformation gradient $\boldsymbol{F}_{\text{pn}}$ and the corresponding elastic part of the deformation gradient, $\boldsymbol{F}_{\text{pn}}^{e}$. These elastic and viscous mechanical potentials are defined, respectively, using a physically-motivated microstructural approach proposed by Arruda and Boyce (also know as the 8-chain model) [2] as

$$\begin{aligned}
\Psi_{\text{mech}}^{e}\left(\boldsymbol{F}\right) = \Psi_{\text{mech}}^{e}\left(\boldsymbol{F}_{\text{pn}}\right) &= \left[1-\phi\right] G^{e} \sum_{k=1}^{K} \frac{C_k}{N_e^{k-1}} \left[I_{1,h}^{k} - 3^{k}\right] \\
\Psi_{\text{mech}}^{v}\left(\boldsymbol{F}, \boldsymbol{F}_{\text{pn}}^{v}\right) = \Psi_{\text{mech}}^{v}\left(\boldsymbol{F}_{\text{pn}}^{e}\right) &= \left[1-\phi\right] G^{v} \sum_{k=1}^{K} \frac{C_k}{N_v^{k-1}} \left[\left[I_{1}^{e}\right]^{k} - 3^{k}\right],
\end{aligned} \tag{18}$$

with G^e and G^v being the shear moduli for the elastic and viscous responses, respectively, N_e and N_v being the number of Kuhn segments per polymer chain for the elastic and viscous networks, respectively, and $I_1^e = \text{tr}\left(\left[\boldsymbol{F}_{\text{pn}}^e\right]^T \boldsymbol{F}_{\text{pn}}^e\right)$. The term ϕ refers to the particles' volume fraction. Moreover, the summation is defined by taking up to five terms, i.e., $[C_1, C_2, C_3, C_4, C_5] = \left[\frac{1}{2}, \frac{1}{20}, \frac{11}{1050}, \frac{19}{7000}, \frac{519}{673750}\right]$. The influence of the magnetic particles on the MAP mechanical response is considered by modifying the first invariant I_1 to $I_{1,h}$ as

$$I_{1,h} = X\left[I_1 - 3\right] + 3 \tag{19}$$

where, $I_1 = \text{tr}\left(\left[\boldsymbol{F}_{\text{pn}}\right]^T \boldsymbol{F}_{\text{pn}}\right)$ and X is an application factor defined as:

$$X = 1 + 0.67g\phi + 1.62\left[g\phi\right]^2 \tag{20}$$

where, g is a factor describing the asymmetric nature of the aggregated clusters, see Alshammari et al. [3]. From the mechanical potentials presented in Eqn (18), mechanical parts (elastic and viscous components) of the first Piola-Kirchhoff stress tensor become

$$\begin{aligned}
\boldsymbol{P}_{\text{mech}}^e &= \frac{\partial \Psi_{\text{mech}}^e}{\partial \boldsymbol{F}} \boldsymbol{F}_{\text{pn}}^{-0} = [1-\phi]\left[2XG^e \sum_{k=1}^{K} \frac{kC_k}{N_e^{k-1}} I_{1,h}^{k-1}\right] \boldsymbol{F}_{\text{pn}} \boldsymbol{F}_{\text{pn}}^{-0} \\
\boldsymbol{P}_{\text{mech}}^v &= \frac{\partial \Psi_{\text{mech}}^v}{\partial \boldsymbol{F}} \boldsymbol{F}_{\text{pn}}^{-0} \boldsymbol{F}_{\text{pn}}^{-v} = [1-\phi]\left[2G^v \sum_{k=1}^{K} \frac{kC_k}{N_v^{k-1}} \left[I_1^e\right]^{k-1}\right] \boldsymbol{F}_{\text{pn}}^e \boldsymbol{F}_{\text{pn}}^{-0} \boldsymbol{F}_{\text{pn}}^{-v}.
\end{aligned} \tag{21}$$

Note that for consistency, these stress tensors must depend on the actual polymeric network deformation gradient instead of the overall MAP deformation gradient. Thus, the mechanical contribution to stress derived directly from the microstructural components and their relative responses.

3.3.2. Magnetic strain energy functions and stress derivations

The magnetic potential per unit volume is defined considering the contribution of two main responses: the dipole-dipole interactions of the magnetisable particles; and the interaction of these magnetised particles with the applied magnetic field. The dipole-dipole interaction contribution to the energy potential, $\Psi_{\text{mag}}^{\text{d-d}}\left(\boldsymbol{F}\right)$, is described following a modification of our recently proposed model for finite strains as (see Garcia-Gonzalez and Hossain [18] for complete derivations and further details)

$$\Psi_{\text{mag}}^{\text{d-d}}\left(\boldsymbol{F}\right) = -\frac{\mu_o}{4\pi}\frac{\phi^2}{\gamma} \sum_{i=1}^{N} \left[\frac{3\left[\left[\boldsymbol{R}\mathbb{M}\right] \cdot \left[\boldsymbol{F}\boldsymbol{R}_i^0\right]\right]\left[\left[\boldsymbol{R}\mathbb{M}\right] \cdot \left[\boldsymbol{F}\boldsymbol{R}_i^0\right]\right]}{\left\|\boldsymbol{F}\boldsymbol{R}_i^0\right\|^5} - \frac{\left[\boldsymbol{R}\mathbb{M}\right] \cdot \left[\boldsymbol{R}\mathbb{M}\right]}{\left\|\boldsymbol{F}\boldsymbol{R}_i^0\right\|^3}\right] \tag{22}$$

where μ_0 is the relative permeability of the vacuum, $\boldsymbol{R}_i^0$ is a dimensionless distance between particles, and the term γ is added to account for the number of particles per representative lattice selected (see [26] for similar approaches). Note that, contrary to our previous model for soft-magnetic particles, the magnetisation vector $\mathbb{M}$ is not a field variable but a constant due to the nature of hard-magnetic particles. In addition, this energy term depends now only on the total deformation gradient $\boldsymbol{F}$, which determines the current relative

position of the magnetic particles with respect to the relative position in the reference configuration (related to $\boldsymbol{R}_i^0$). Regarding the contribution of the hard-magnetic particles' interaction with the applied magnetic field, internal torques will be generated as the particles will try to align along the applied field direction. This contribution can be written as

$$\Psi_{\text{mag}}^{\text{z}}\left(\boldsymbol{F},\mathbb{B}\right)=-\boldsymbol{R}\mathbb{M}\cdot\boldsymbol{F}\mathbb{B}. \tag{23}$$

Note that the formulation used by Zhao and co-authors [54] has been modified to account for the consideration that magnetisation depends only on the rigid body rotation but not on the stretch part of the deformation gradient. This aspect is important as here $\mathbb{M}$ represents the magnetisation of the particles (which does not stand for significant deformations), and not the homogenised magnetisation of the composite. The magnetic part due to dipole-dipole interactions of the first Piola-Kirchhoff stress tensor becomes

$$\boldsymbol{P}_{\text{mag}}^{\text{d-d}}=\frac{\partial\Psi_{\text{mag}}^{\text{d-d}}}{\partial\boldsymbol{F}}=-\frac{\mu_o}{4\pi}\frac{\phi^2}{\gamma}\sum_i\left[\frac{6\left[\left[\boldsymbol{R}\mathbb{M}\right]\cdot\left[\boldsymbol{F}\boldsymbol{R}_i^0\right]\right]\left[\left[\boldsymbol{R}\mathbb{M}\right]\otimes\boldsymbol{R}_i^0\right]}{\left\|\boldsymbol{F}\boldsymbol{R}_{\boldsymbol{i}}^{\boldsymbol{0}}\right\|^5}\right.$$
$$\left.-\frac{15\left[\left[\boldsymbol{R}\mathbb{M}\right]\cdot\left[\boldsymbol{F}\boldsymbol{R}_i^0\right]\right]\left[\left[\boldsymbol{R}\mathbb{M}\right]\cdot\left[\boldsymbol{F}\boldsymbol{R}_{\boldsymbol{i}}^{\boldsymbol{0}}\right]\right]\left[\boldsymbol{R}_i^0\otimes\boldsymbol{R}_i^0\right]\boldsymbol{F}}{\left\|\boldsymbol{F}\boldsymbol{R}_i^0\right\|^7}+\frac{3\left[\left[\boldsymbol{R}\mathbb{M}\right]\cdot\left[\boldsymbol{R}\mathbb{M}\right]\right]\left[\boldsymbol{R}_i^0\otimes\boldsymbol{R}_i^0\right]\boldsymbol{F}}{\left\|\boldsymbol{F}\boldsymbol{R}_i^0\right\|^5}\right]. \tag{24}$$

Now, the remaining magnetic part of the first Piola-Kirchhoff stress tensor becomes

$$\boldsymbol{P}_{\text{mag}}^{\text{z}}=\frac{\partial\Psi_{\text{mag}}^{\text{h-m}}}{\partial\boldsymbol{F}}=-\mathbb{B}\otimes\boldsymbol{R}\mathbb{M}. \tag{25}$$

3.3.3. Viscous flow rule

To complete the formulation, the evolution of the viscous part of the deformation gradient $\boldsymbol{F}_{\text{pn}}^v$ must be consistently defined. To this end, we take a linear viscous model from previous works relating the viscous deformation rate tensor $\boldsymbol{D}_{\text{pn}}^v$ to the viscous stress as [16, 17]

$$\boldsymbol{D}_{\text{pn}}^v=\boldsymbol{F}_{\text{pn}}^e\dot{\boldsymbol{F}}_{\text{pn}}^v\boldsymbol{F}_{\text{pn}}^{-v}\boldsymbol{F}_{\text{pn}}^{-e}=\frac{\boldsymbol{\sigma}_{\text{mech}}^v}{\sqrt{2}\eta} \tag{26}$$

where, η is the polymer viscosity and $\boldsymbol{\sigma}_{\text{m}}^v$ is the viscous contribution to the Cauchy stress tensor $\boldsymbol{\sigma}_{\text{mech}}^v=\boldsymbol{P}_{\text{mech}}^v\boldsymbol{F}^T$.

3.4. Numerical computation of the initial pre-stretch field

Following the discussion presented in Section 3.1, hMAPs manufactured under the application of a magnetic field during the curing process yield dipole-dipole interactions between the magnetised particles. Therefore, at the reference configuration without the application of any mechanical and/or magnetic external fields, the fulfilment of the mechanical balance requires a stress contribution from the polymeric network. This contribution results in a pre-deformation state of the network (given by $\boldsymbol{F}_{\text{pn}}^0$). In this section, we present a numerical scheme to compute the $\boldsymbol{F}_{\text{pn}}^0$ tensor. For this, the total first Piola-Kirchhoff stress tensor, without any mechanical and/or magnetic external fields, is computed as

$$\boldsymbol{P}|_{t=0} = \left[\boldsymbol{P}^{e}_{\text{mech}} + \boldsymbol{P}^{v}_{\text{mech}} + \boldsymbol{P}^{\text{d-d}}_{\text{mag}} + \boldsymbol{P}^{\text{z}}_{\text{mag}} - p\boldsymbol{F}^{-T}\right]|_{t=0} = \boldsymbol{P}^{e}_{\text{mech}}|_{\boldsymbol{F}=\boldsymbol{I}} + \boldsymbol{P}^{v}_{\text{mech}}|_{\boldsymbol{F}=\boldsymbol{F}^{v}_{\text{pn}}=\boldsymbol{I}} + \boldsymbol{P}^{\text{d-d}}_{\text{mag}}|_{\boldsymbol{F}=\boldsymbol{I}} - p\boldsymbol{I}. \tag{27}$$

In addition, the hMAP must be in mechanical equilibrium when considering null external forces so that

$$\boldsymbol{P}|_{t=0} = \boldsymbol{0}. \tag{28}$$

To ensure such a strong consistency condition, we devise a Newton-Raphson algorithm that, depending on the residual magnetisation of the particles and their spatial distribution within the MAP, provides the pre-deformation tensor $\boldsymbol{F}^{0}_{\text{pn}}$ of the polymeric network. For that, we define the residual as

$$\boldsymbol{Res} = \boldsymbol{P}^{e}_{\text{mech}}|_{\boldsymbol{F}=\boldsymbol{I}} + \boldsymbol{P}^{v}_{\text{mech}}|_{\boldsymbol{F}=\boldsymbol{F}^{v}_{\text{pn}}=\boldsymbol{I}} + \boldsymbol{P}^{\text{d-d}}_{\text{mag}}|_{\boldsymbol{F}=\boldsymbol{I}} - p\boldsymbol{I} = \boldsymbol{0}. \tag{29}$$

The stiffness or iteration matrix, can be expressed in index notation as

$$K_{iJKL} = \frac{\partial Res_{iJ}}{\partial F^{0}_{pn,KL}}. \tag{30}$$

To compute the components of the stiffness matrix, due to the complexity of the stress formulation, we adopt a numerical approximation scheme following the work of Miehe [38] and Johnsen et al. [27]. In this regard, $\boldsymbol{F}^{0}_{\text{pn}}$ is perturbed as

$$\hat{\boldsymbol{F}}^{0,(KL)}_{\text{pn},\pm} = \boldsymbol{F}^{0}_{\text{pn}} \pm \Delta\boldsymbol{F}^{0,(KL)}_{\text{pn},\pm} \tag{31}$$

where,

$$\Delta\boldsymbol{F}^{0,(KL)}_{\text{pn},\pm} = \pm\frac{\epsilon}{2}\left[(\boldsymbol{e}_K \otimes \boldsymbol{e}_L)\,\boldsymbol{F}^{0}_{\text{pn}} + (\boldsymbol{e}_L \otimes \boldsymbol{e}_K)\,\boldsymbol{F}^{0}_{\text{pn}}\right] \tag{32}$$

with ϵ being the perturbation coefficient set to 10^{-8} and $\boldsymbol{e}_K$ being the Cartesian base vectors with $K = 1, 2, 3$. Therefore, using a central difference scheme, the stiffness matrix components are computed as

$$K_{iJKL} = \frac{P_{iJ}\left(\hat{\boldsymbol{F}}^{0,(KL)}_{\text{pn},+}\right) - P_{iJ}\left(\hat{\boldsymbol{F}}^{0,(KL)}_{\text{pn},-}\right)}{2\epsilon}. \tag{33}$$

4. Computational insights from the microstructural-based model

This section analyses, from theoretical bases, the importance of the dipole-dipole interactions in the overall response of hMAPs. We first evaluate the influence of such dipole-dipole interactions on the MAP pre-stretch. Secondly, the effects of the dipole-dipole interactions during MAP deformation under a null external magnetic field are analysed. Finally, we present a comparison of the different mechanical and magnetic contributions to the MAP response under various magneto-mechanically coupled conditions. For all simulations presented herein, we use the material parameters summarised in Table 1, which are directly taken from the literature [45, 54, 18, 53]. It is also important to highlight that we aim at reproducing hMAPs that are magnetised during the curing process so that the composite reaches an equilibrium state under free-stress condition where the polymeric network balances the dipole-dipole interactions of the magnetic particles. In such situations, the particles are expected to align along the externally applied magnetic field. There-

fore, we assume ideal chain-like distributions of the particles within the polymeric matrix. For a detailed classification of particle arrangements and its implications within the MAP, see our previous work [18]. In addition, note that the dipole-to-dipole interactions are determined by the magnetisation of the particles and the distance between them. Therefore, for the same particles-type (i.e., size and remanent magnetisation), an increase in volume fraction leads to smaller distances resulting into higher interaction forces. The simulations have been conducted for a particle content of $\phi = 0.3$. Moreover, to analyse the effect of this parameter and its influence at lower values (Kim and co-authors [31, 32] reported experimental volume fractions around $\phi = 0.2$), we perform simulations evaluating the influence of ϕ on the pre-stretch (see Figure A1 in Appendix).

Table 1: Constitutive parameters used in the simulations. The parameters for the polymeric matrix contribution are taken from [45, 18], and the parameters for the magnetic particles are taken from [54, 53]. Note that we have considered two different values for the remanent magnetisation vector $\mathbb{M}$, both values directly taken from experimental data in the literature, to analyse the influence of such an important parameter for the proposed model.

Mechanical parameters for 8-chain model					
$G^e\,(kPa)$	$N_e\,(-)$	$G^v\,(kPa)$	$N_v\,(-)$	$\eta\,(Pas)$	$g\,(-)$
8	12	8	5	2000	10
Magnetic parameters					
$\lvert\mathbb{M}\rvert\,(kA/m)$	$\mu_r\,(-)$	$\mu_o\,(H/m)$			
205 [54]; 600 [53]	1.05	$4\pi 10^{-7}$			

4.1. Evaluation of the influence of polymeric pre-stretch

At first, the consistency of the pre-stretch approach and its consequences are analysed in this section. For that, we simulate uniaxial tensile deformation processes at two different strain rates under a null external magnetic field, and considering two different realistic initial magnetisations (see discussions in [54, 53]). Note that the magnitude of such a remanent magnetisation, along with the stiffness of the polymeric network, will determine the influence of particles' dipole-dipole interactions. The proposed simulations are conducted considering and neglecting the initial pre-stretch, see Figure 2. It presents the evolution of the MAP mechanical response by plotting stress versus composite stretch (related to $\boldsymbol{F}$). In these simulations, the dipole-dipole interaction due to the remanent magnetisation of the particles is considered. Such magnetic internal forces lead to an internal stress within the MAP that, in the case of an initial stress-free state, must result into a pre-stretch of the polymeric network so that the mechanical balance is fulfilled. The magnitude of the polymeric pre-stretch depends on the magnitude of the magnetic interactions and, therefore, on the initial magnitude of the magnetisation (Figure 2b). If this polymeric pre-stretch is considered, the stress of the overall MAP at initial stage is zero (Figure 2). However, if this is not considered, a clear offset of these curves is observed indicating an initial pre-stress state within the MAP (Figure 2). Moreover, the predictions show an equivalent increase in the stiffness for both cases from increasing strain rate as a result of viscous contributions (Figure 2a).

When performing the same analysis under a pure shear deformation, no significant differences are observed for a remanent magnetisation of $|\mathbb{M}| = 205kA/m$ (Figure 3a). However, if the remanent magnetisation is higher, $|\mathbb{M}| = 600kA/m$, significant changes are observed due to longitudinal pre-stretch, although no shear pre-stretch is appreciated for the conditions tested (Figure 3b). Regarding the influence of strain rate, we can observe a similar increase in the stiffness for higher loading rates as in the previous simulations under tensile loading.

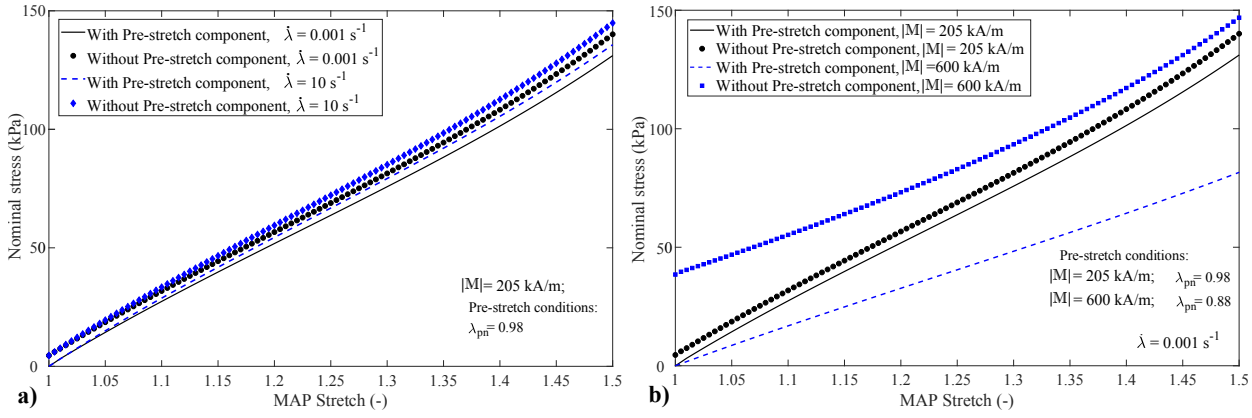

Figure 2. Model predictions under a uniaxial tensile mechanical loading for the proposed formulation accounting for an equilibrium polymeric network component ($\boldsymbol{F}_{\text{pn}}$) and without considering such a pre-stretch state. Null external magnetic field is applied. a) Dependence on strain rate for $|\mathbb{M}| = 205kA/m$; b) dependence on the remanent magnetisation for a strain rate of $0.001s^{-1}$.

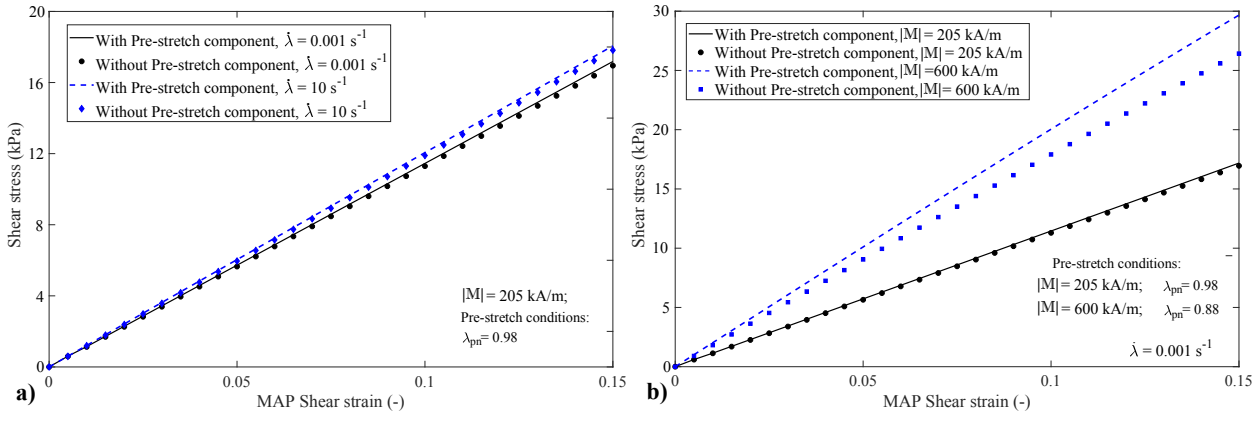

Figure 3. Model predictions under shear mechanical loading for the proposed formulation accounting for an equilibrium polymeric network component ($\boldsymbol{F}_{\text{pn}}$) and without considering such a pre-stretch state. Null external magnetic field is applied. a) Dependence on strain rate for $|\mathbb{M}| = 205kA/m$; b) dependence on the remanent magnetisation for a shear strain rate of $0.001s^{-1}$.

4.2. Evaluation of the influence of dipole-dipole interactions

This second study evaluates the influence of dipole-dipole interactions under a null external magnetic field during mechanical deformation. The presence of magnetised particles (residual magnetisation due to the hard-magnetic nature) results into magnetic dipole-dipole forces. These forces do not only depend on the residual magnetisation of the particles but also on their relative distances and distribution, see Equation 24. Therefore, if the MAP experiences any mechanical deformation process, the relative distances and orientation of the particles are changed, leading to an alteration in the dipole-dipole interactions. This effect has indirectly been demonstrated in molecular dynamic simulations and directly relates to the nature of magnetised particles and dipole-dipole interactive forces [44]. It must be noted that most of the current continuum modelling approaches do not account for such dipole-dipole effects, neither the macroscopic models [54] nor the microstructural ones [53]. To evaluate such effects, we take a uniaxial tensile deformation test as the reference one, under null external magnetic field, in which the magnetic particles are defined with null residual magnetisation (see Figure 4). The simulation is compared with the same scenario but defining

two different initial residual magnetisations in the particles. In the latter cases, in order to impose initial free-stress, a pre-stretch of the polymeric network must be computed and accounted for. The results shown in Figure 4 highlight the importance of accounting for dipole-dipole interactions during the deformation process of a hMAP under a null external magnetic field. While previous approaches in the literature (i.e., [54, 53]) are accurate for small deformations, they can present certain limitations when higher deformations are reached. In addition, the consideration of actual magnetisation dependent on the rigid body rotation but not on the material stretch (Equation 23), according to previous experimental and numerical observations [39, 15, 40], also influences significantly the model predictions at large deformations.

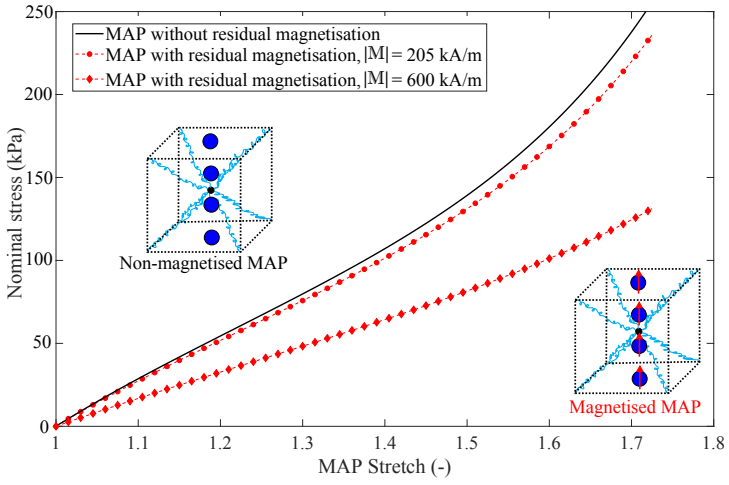

Figure 4. Model predictions for magnetised and non-magnetised MAPs. A null external magnetic field is applied while two different remanent magnetisations are considered and a strain rate of $0.001s^{-1}$ is imposed. Note that this figure shows the importance of accounting for dipole-dipole interactions to accurately define the mechanical behaviour under a null external magnetic field.

In order to interpret the previous results further, we provide the evolution of the different stress components during the deformation process (Figure 5). For hMAP stretch equal to 1, i.e., initial stress-free condition, it can be observed the balance between the magnetic stress due to the dipole-dipole interactions and the mechanical stress due to the polymeric network pre-stretch. As the hMAP (total) stretch increases, the mechanical contribution due to the polymeric network deformation increases; while the magnetic contribution decreases as a consequent of larger distances between magnetic particles in turn leading to smaller interaction forces. Overall, the dipole-dipole contribution to the stress is only significant in the first stages of the deformation process. However, the associated pre-stretch of the polymeric network has further implications in the stress response due to the offset between the hMAP and polymeric matrix effective deformations.

4.3. Evaluation of the full magneto-mechanical coupling

In this section, we present the model predictions accounting for all the magneto-mechanical responses and their relative role. To this end, we consider two external magnetic conditions: i) a null initial external magnetic field followed by the application of a constant magnetic field rate until reaching $|\mathbb{B}| = 0.2T$ longitudinally to the particles' chain-like distribution and opposite to the particles' magnetisation direction; ii) a constant external magnetic field of $|\mathbb{B}| = 0.2T$ aligned to the particles' chain-like distribution and opposite to the particles' magnetisation direction. In parallel to the external magnetic field, we simulate a mechanical

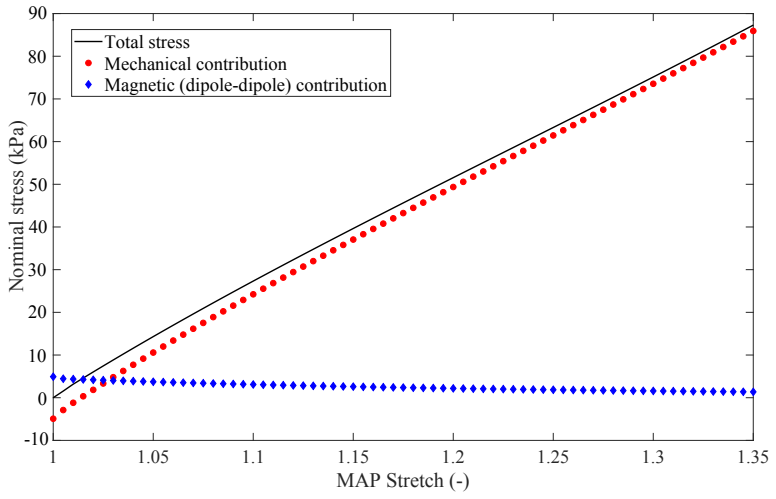

Figure 5. Decomposition of the MAP stress into mechanical and magnetic dipole-dipole interaction components. A null external magnetic field is applied, while $|\mathbb{M}| = 205kA/m$ is considered.

deformation under uniaxial tension along the magnetic field direction. These numerical results are shown in Figure 6.

The most relevant observation from Figure 6 is that both mechanical and dipole-dipole interaction contributions are modulated by the deformation of the hMAP. However, the stress contribution from the Zeeman effect does not depend on the hMAP stretch state. The mechanical contribution is determined by the deformation state of the polymeric network and its application rate. In this regard, the deformation of the hMAP along with the initial pre-stretch of the polymeric matrix determine the actual stretch of the polymeric chains. As these chains are stretched, the hMAP experiences an increase in stress following Equation 21. Note that due to the viscous nature of the polymeric matrix, this stress contribution also depends on the strain rate and strain history. Moreover, the dipole-dipole interaction contribution to the stress directly depends on the relative distance between particles. Therefore, the deformation of the hMAP leads to changes in such distances modulating its stress contribution according to Equation 24. For the hard-magnetic response and in accordance with previous experimental and numerical works [39, 15, 40], we have assumed that the magnetisation does not depend on the material stretch but only on the rotation. Therefore, it is expected that the hard-magnetic contribution to hMAP stress depends on the residual magnetisation of the particles, their volume fraction and spatial orientation (accounting for rigid body rotations), but not on the hMAP stretch.

5. Conclusions

In this work, we present a microstructural-based constitutive model for hard-magnetic MAPs (hMAPs). More precisely, we aim at overcoming the current modelling limitations to describe the full magneto-mechanical response of hMAPs that are magnetised during the curing process. In such a scenario and under free-stress conditions of the post-cured MAP, the composite reaches an equilibrium state where the polymeric network balances the dipole-dipole interactions of the magnetic particles. The formulation is developed for finite strain settings following a thermodynamically consistent approach. The model describes the overall magneto-mechanical response of the MAP considering the specific contributions of its

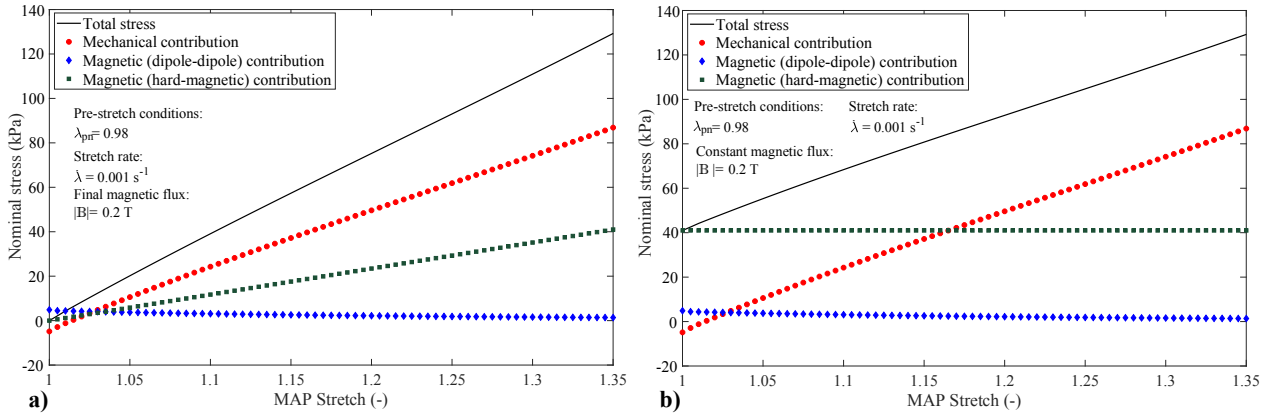

Figure 6. Decomposition of the MAP stress into mechanical, magnetic dipole-dipole interaction, and hard magnetic components where $|\mathbb{M}| = 205kA/m$ is considered. An external magnetic field is applied in the magnetisation direction of the particles: a) at a constant rate until reaching a final magnitude of 0.2T opposite to the particles' magnetisation direction; b) constant during the whole deformation process and with a magnitude of 0.2T opposite to the particles' magnetisation direction.

phases. Thus, within a single framework, the constitutive model accounts for polymeric network pre-stretch, dipole-dipole interactions, Zeeman effect and viscous mechanisms. After presenting the formulation and its numerical implementation, we use the model to analyse, from theoretical bases, the importance of dipole-dipole interactions in the overall response of hMAPs. The numerical results reveal that a pre-deformation of the polymeric network is required to reach consistent mechanical balance in the presence of magnetised particles. This pre-deformation state of the polymeric matrix results are important if the model is directly fed from properties of the microstructural components. In addition, the alteration of the distances between particles during the MAP deformation leads to changes in the dipole-dipole interactions affecting the overall response of the composite. This effect is shown important especially when simulating the mechanical response of the magnetised MAP under a null external magnetic field.

Acknowledgement

D.G.G. acknowledges support from the Talent Attraction grant (CM 2018 - 2018-T2/IND-9992) from the Comunidad de Madrid, and support from the European Research Council (ERC) under the European Union's Horizon 2020 research and innovation programme (grant agreement No. 947723, project 4D-BIOMAP). M. H. acknowledges the funding through an EPSRC Impact Acceleration Award (EP/R511614/1).

Appendix A. Evaluation of particles' volume fraction and residual magnetisation on MAP pre-stretch

This appendix analyses the effect of the particles' volume fraction ϕ and residual magnetisation of the particles $|\mathbb{M}|$ on the pre-stretch. Related numerical results are presented in Figure A.1. It can be observed that higher volume fractions lead to smaller distances between particles and, therefore, to higher pre-stretch due to dipole-dipole interactions. Moreover, an increase in the residual magnetisation results in stronger magnetic forces between particles leading to an increase in the pre-stretch. A relevant recent work is due to Yan et al. [50], in which the authors developed a robust mechanism to control the buckling strength of (hard-magnetic) shells in a dynamic fashion by means of magneto-mechanical coupling. The authors

conducted experiments showing that low particle volume fraction (7%) does not affect the overall performance. These results are consistent with our numerical simulations (Figure A.1) where, depending on the particles' magnetisation, show that low particles' volume fractions lead to negligible pre-stretches and lower magneto-mechanical coupling.

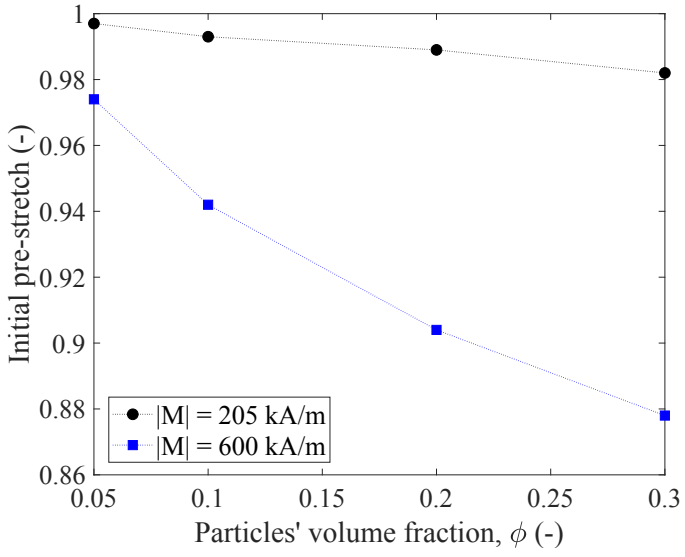

Figure A.1. Influence of the initial pre-stretch due to dipole-to-dipole interactions on particles' volume fraction and residual magnetisation.

References

[1] Alapan, Y., Karacakol, A. C., Guzelhan, S. N., Isik, I., Sitti, M., 2020. Reprogrammable shapemorphing of magnetic soft machines. Science advances, 6:eabc6414.

[2] Arruda, E.M., Boyce, M.C. 1993. A three-dimensional constitutive model for the large stretch behavior of rubber elastic materials. Journal of Mechanics and Physics of Solids, 41:389-412

[3] Alshammari, B. A., Al-Mubaddel, F.S., Karim, M. R., Hossain, M., Al-Mutairi, A.S., Wilkinson, A.N. 2019. Addition of graphite filler to enhance electrical, morphological, thermal, and mechanical properties in 500 poly (ethylene terephthalate): Experimental characterization and material modeling, Polymers 11 (9):1411

[4] Bastola, A. K., Hossain, M., 2020. A review on magneto-mechanical characterizations of magnetorheological elastomers, Composites Part B: Engineering, 200, 108348.

[5] Böse, H., 2007. Viscoelastic properties of silicone-based magnetorheological elastomers. Int. J. Mod. Phys. B 21, 4790–4797.

[6] Bustamante, R., Shariff, M. H. B. M., Hossain, M., 2021. Mathematical formulations for elastic magneto-electrically coupled soft materials at finite strains: Time-independent processes, International Journal of Engineering Science, 159: 103429

[7] Bica, I., 2012. The influence of the magnetic field on the elastic properties of anisotropic magnetorheological elastomers. J. Ind. Eng. Chem. 18, 1666–1669.

[8] Boczkowska, A., Awietjan, S.F., 2009. Smart composites of urethane elastomers with carbonyl iron. J. Mater. Sci. 44, 4104–4111.

[9] Boczkowska, A., Awietjan, S.F., 2012. Microstructure and properties of magnetorheological elastomers. In Advanced Elastomers-Technology, Properties and Applications, Ed. Boczkowska, A. DOI:10.5772/2784 pp.147–180.

[10] Coleman B D, M. E. Gurtin, Thermodynamics with internal state variables, Journal of Chemical Physics, 47:597-613, 1967

[11] Coquelle, E., Bossis, G., 2005. Magnetostriction and piezoresistivity in elastomers filled with magnetic particles, Journal of Advanced Science, 17:132-133

[12] Diguet, G., Beaugnon, E., Cavaille, J. Y., 2010. Shape effect in the magnetostriction of ferromagnetic composite, Journal of Magnetism and Magnetic Materials, 322:3337

[13] A. Dorfmann, R.W. Ogden, Some problems in nonlinear magnetoelasticity, Z. Angew. Math. Phys. 56 (4): 718–745, 2005

[14] Dorfmann A, R. W. Ogden, Nonlinear magnetoelastic deformations of elastomers, Acta Mechanica, 167(1-2):13-28, 2004

[15] Danas, K., Kankanala, S. V., Triantafyllidis, N., 2012. Experiments and modelling of iron-particled-filled magnetorheological elastomers. J. Mech. Phys. Solids 60(1), 120–138.

[16] Garcia-Gonzalez, D., 2019. Magneto-visco-hyperelasticity for hard-magnetic soft materials: theory and numerical applications. Smart Materials and Structures, 28:085020

[17] Garcia-Gonzalez, D., Landis, C.M., 2020. Magneto-diffusion-viscohyperelasticity for magneto-active hydrogels: rate dependences across time scales. Journal of the Mechanics and Physics of Solids, 139:103934.

[18] Garcia-Gonzalez, D., Hossain, M., 2021. A microstructural-based approach to model magneto-viscoelastic materials at finite strains. International Journal of Solids and Structures, 208-209:119-132.

[19] Garcia-Gonzalez, D., Moreno MA, Valencia L, Arias A, Velasco D. Influence of Elastomeric Matrix and Particle Volume Fraction on the Mechanical Response of Magneto-Active Polymers. Composites Part B: Engineering, 2021 215 (June): 108796. https://doi.org/10.1016/j.compositesb.2021.108796.

[20] Griffiths D J, Introduction to Electrodynamics, 3rd ed. Prentice Hall (1998)

[21] Haldar, K., Kiefer, B., Menzel, A., 2016 Finite element simulation of rate-dependent magneto-active polymer response, Smart Materials and Structures, 25 : 104003

[22] Hossain, M., Saxena, P., Steinmann, P., 2015. Modelling the mechanical aspects of the curing process of magneto-sensitive elastomeric materials, International Journal of Solids and Structures 58: 257-269

[23] Hossain, M., Saxena, P., Steinmann, P., 2015. Modelling the curing process in magneto-sensitive polymers: Rate-dependence and shrinkage, International Journal of Non-Linear Mechanics, 74: 108-121

[24] Hossain, M., Chatzigeorgiou, G., Meraghni, F., Steinmann, P., 2015. A multi-scale approach to model the curing process in magneto-sensitive polymeric materials, International Journal of Solids and Structures, 69-70:34-44

[25] Hu, W., Zhan, G., Mastrangeli, M., Sitti, M., 2018. Small-scale soft-bodied robot with multimodal locomotion, Nature, 554:81-85

[26] Ivaneyko, D., Toshchevikov, V., Saphiannikova, M., Heinrich, G., 2012. Effects of particle distribution on mechanical properties of magneto-sensitive elastomers in a homogeneous magnetic field. Condensed Matter Physics 15, 33601

[27] Johnsen, J., Clausen, A.H., Grytten, F., Benallal, A., Hopperstad, O.S., 2019. A thermo-elasto-viscoplastic constitutive model for polymers, Journal of the Mechanics and Physics of Solids, 124:681-701.

[28] Kadapa, C., Hossain, M., 2020. A linearised consistent mixed displacement-pressure formulation for hyperelasticity, Mechanics of Advanced Materials and Structures, In Press, DOI: 10.1080/15376494.2020.1762952

[29] Kankanala, S.V., Triantafyllidis, N., 2004. On finitely strained magnetorheological elastomers. J. Mech. Phys. Solids 52, 2869–2908.

[30] Kalina, K. A., Brummund, J., Metsch, P., Kaestner, M., Borin, D. Y., Linke, J. M., Odenbach, S. 2017, Smart Materials and Structures, 26(10):105019

[31] Kim, Y., Yuk, H., Zhao, R., Chester, S. A., Zhao., X., 2018. Printing ferromagnetic domains for untethered fast-transforming soft materials, Nature 558 (7709): 274-27

[32] Kim, Y., Parada, G. A., Liu, S., and Zhao, X., 2019. Ferromagnetic soft continuum robots, Science Robotics, 4(33), p. eaax7329.

[33] Landau, L.D., Lifshitz, E.M., 1963. Electrodynamics of continuous media.

[34] Lee, M., Park, T., Kim, C., Park, S. M., 2020. Characterization of a magneto-active membrane actuator comprising hard magnetic particles with varying crosslinking degrees, Materials & Design, 195:108921

[35] Lum, G. Z., Ye, Z., Dong, X., Marvi, H., Erin, O., Hu, W., and Sitti, M., 2016. Shape-programmable magnetic soft matter. Proceedings of the National Academy of Sciences, 113(41), pp. E6007-E6015.

[36] Maugin, G.A., 1988. Continuum Mechanics of Electromagnetic Solids, North Holland, Amsterdam.

[37] Mehnert, M., Hossain, M., Steinmann, P. 2017. Towards a thermo-magneto-mechanical coupling framework for magneto-rheological elastomers, International Journal of Solids and Structures, 128:117-132

[38] Miehe, C., 1996. Numerical computation of algorithmic (consistent) tangent moduli in large-strain computational inelasticity, Comput. Methods Appl. Mech. Eng., 134:223-240

[39] Mukherjee, D., Bodelot, L., Danas, K., 2020. Microstructurally-guided explicit continuum models for isotropic magnetorheological elastomers with iron particles, International Journal of Non-Linear Mechanics, 120:103380.

[40] Mukherjee, D., Rambausek, M., Danas, K., 2021. An explicit dissipative model for isotropic hard magnetorheological elastomers, Journal of the Mechanics and Physics of Solids 151:104361.

[41] Nadzharyan, T.A., Stolbov, O.V., Raikher, Y.L, Kramarenko, E.Y., 2019. Field-induced surface deformation of magnetoactive elastomers with anisometric fillers: a single-particle model, Soft Matter, 15:9507–9519.

[42] de Souza Neto, E. D., Peric, D., Owen, D. R. J. Computational methods for plasticity: theory and applications, Wiley, 2008

[43] Ren, Z., Hu, W., Dong, X., Sitti, M. 2019., Multi-functional soft-bodied jellyfish-like swimming, Nature Communications, 10:2703.

[44] Sanchez, P.A., Stolbov, O.V., Kantorovich, S.S., Raikher, Y.L., 2019. Modeling the magnetostriction effect in elastomers with magnetically soft and hard particles. Soft Matter, 15:7145.

[45] Soria-Hernandez, C.G., Palacios-Pineda, L.M., Elias-Zuniga, A., Perales-Martinez, I.A., Martinez-Romero, O., 2019. Investigation of the Effect of Carbonyl Iron Micro-Particles on the Mechanical and Rheological Properties of Isotropic and Anisotropic MREs: Constitutive Magneto-Mechanical Material Model. Polymers, 11(10):1705

[46] Schuemann, M. Borin, D. Y., Morich, J., Odenbach, S. 2020 Reversible and non-reversible motion of NdFeB-particles in magnetorheological elastomers, Journal of Intelligent Materials Systems and Structures, DOI:10.1177/1045389X20949703

[47] Wang, L., Kim, Y., Guo, G.F., Zhao, X., 2020. Hard-magnetic elastica. Journal of the Mechanics and Physics of Solids, 142: 104045.

[48] Wang, L., Zheng, D., Harker, P., Patel, A.B., Guo, C.F., Zhao, X., 2021. Evolutionary design of magnetic soft continuum robots. Proceedings of the National Academy of Sciences, 118:21.

[49] Wu, S., Hamel, C.M., Ze, Q., Yang, F., Qi, H.J. and Zhao, R. (2020), Evolutionary Algorithm-Guided Voxel-Encoding Printing of Functional Hard-Magnetic Soft Active Materials. Adv. Intell. Syst., 2: 2000060.

[50] Yan, D., Pezzulla, M., Cruveiller, L. et al., 2021. Magneto-active elastic shells with tunable buckling strength. Nat Commun, 12, 2831.

[51] Ye, H., Li, Y., Zhang, T., 2020. Magttice: A Lattice Model for Hard-Magnetic Soft Materials, Soft Matter, DOI: 10.1039/D0SM01662D.

[52] Ze, Q., Kuang, X., Wu, S., Wong, J., Montgomery, S. M., Zhang, R., Kovitz, J. M., Yang, F., Qi, H. J., and Zhao, R., 2020. Magnetic Shape Memory Polymers with Integrated Multifunctional Shape Manipulation, Advanced Materials, 32(4), p. 1906657.

[53] Zhang, R., Wu, S., Qiji, Z., Zhao, Z., 2020. Micromechanics Study on Actuation Efficiency of Hard-Magnetic Soft Active Materials, Journal of Applied Mechanics, 87:091008.

[54] Zhao, R., Kim, Y., Chester, A. S., Sharma, P., Zhao, X., 2019. Mechanics of hard-magnetic soft materials, Journal of the Mechanics and Physics of Solids, 124: 244-263